Pituitary adenylate cyclase-activating polypeptide is a sympathoadrenal neurotransmitter involved in catecholamine regulation and glucohomeostasis

Carol Hamelink*, Olga Tjurmina†, Ruslan Damadzic*, W. Scott Young‡, Eberhard Weihe§, Hyeon-Woo Lee*, and Lee E. Eiden*¶

Sections on *Molecular Neuroscience and ‡Neural Gene Expression, Laboratory of Cellular and Molecular Regulation, and †Laboratory of Clinical Science, National Institute of Mental Health, Bethesda, MD 20892; and §Department of Anatomy and Cell Biology, Philipps University, D-35037 Marburg, Germany

Communicated by Julius Axelrod, National Institutes of Health, Bethesda, MD, November 14, 2001 (received for review October 1, 2001)

The adrenal gland is important for homeostatic responses to metabolic stress: hypoglycemia stimulates the splanchnic nerve, epinephrine is released from adrenomedullary chromaffin cells, and compensatory glucogenesis ensues. Acetylcholine is the primary neurotransmitter mediating catecholamine secretion from the adrenal medulla. Accumulating evidence suggests that a secretin-related neuropeptide also may function as a transmitter at the adrenomedullary synapse. Costaining with highly specific antibodies against the secretin-related neuropeptide pituitary adenylate cyclase-activating peptide (PACAP) and the vesicular acetylcholine transporter (VAChT) revealed that PACAP is found in nerve terminals at all mouse adrenomedullary cholinergic synapses. Mice with a targeted deletion of the PACAP gene had otherwise normal cholinergic innervation and morphology of the adrenal medulla, normal adrenal catecholamine and blood glucose levels, and an intact initial catecholamine secretory response to insulin-induced hypoglycemia. However, insulin-induced hypoglycemia was more profound and longer-lasting in PACAP knock-outs, and was associated with a dose-related lethality absent in wild-type mice. Failure of PACAP-deficient mice to adequately counterregulate plasma glucose levels could be accounted for by impaired long-term secretion of epinephrine, secondary to a lack of induction of tyrosine hydroxylase, normally occurring after insulin hypoglycemia in wild-type mice, and a consequent depletion of adrenomedullary epinephrine stores. Thus, PACAP is needed to couple epinephrine biosynthesis to secretion during metabolic stress. PACAP appears to function as an ''emergency response'' cotransmitter in the sympathoadrenal axis, where the primary secretory response is controlled by a classical neurotransmitter but sustained under paraphysiological conditions by a neuropeptide.

The adrenal medulla has been used extensively as a model for understanding basic features of neurotransmission and transsynaptic regulation, because of the simplicity of its synaptic inputs and the physiological importance and ease of measurement of catecholamine secretion as a final output (1). Recently, the adrenomedullary synapse has been the focus of analysis of the functional meaning of classical neurotransmitter and neuropeptide coexpression and corelease at mammalian synapses (2). Acetylcholine is the primary neurotransmitter mediating catecholamine secretion from the adrenal medulla (3). A second noncholinergic neurotransmitter also is thought to be involved in sympathoadrenal function because acetylcholine, or cholinergic agonists alone, cannot mimic the prolonged secretion and robust stimulation of catecholamine biosynthesis elicited by electrical stimulation of the splanchnic innervation of the adrenal medulla (4–7). It has been proposed that pituitary adenylate cyclase-activating peptide (PACAP) or a PACAP-related neuropeptide acts as a cotransmitter with acetylcholine at the adrenomedullary synapse, based on neuroanatomical evidence obtained *in vivo* and pharmacological and physiological evidence obtained *in vitro* and *ex vivo* (8–11).

Vasoactive intestinal polypeptide (VIP) and PACAP are members of the same neuropeptide superfamily (12), and both have been suggested as splanchnicoadrenomedullary cotransmitters. Electrical stimulation of the splanchnic nerve releases VIP, which can elicit catecholamine secretion from perfused adrenal and in cultured chromaffin cells (9). PACAP is a more potent secretagogue of catecholamines from chromaffin cells than VIP (13–17). Both VIP and PACAP have been proposed as autonomic neurotransmitters (9, 10). However, it has not yet been possible to assign a physiological role to either peptide in adrenomedullary function *in vivo*.

Elimination of the PACAP-preferring PAC1 receptor in mice leads to a relatively mild phenotype associated with a slight postprandial hyperglycemia and a diminished insulin secretory response after glucose infusion (18). These receptor knock-out mice have not yet been informative about the role of PACAP in adrenomedullary neurotransmission, perhaps because chromaffin cells *in vivo* possess multiple PACAP- and VIP-responsive receptors (8). Assessing the role of PACAP (or VIP) at the adrenomedullary synapse is therefore likely to require the disruption of multiple receptors or the neuropeptide genes themselves.

Thus, despite progress in elucidating neuroanatomical and pharmacological details necessary to assess the role of PACAP-related peptides as adrenomedullary cotransmitters, acetylcholine/neuropeptide cotransmission in the adrenal medulla is still not functionally understood. Here, we investigate the neuroanatomical localization of PACAP at adrenomedullary synapses, and the physiological role of PACAP cotransmission by using direct *in vivo* measurement of catecholamine secretion from the adrenal, in wild-type and PACAP-deficient mice. Our results indicate that the development, morphology, and basal function of the adrenal medulla do not require PACAP but that PACAP is required for catecholamine secretion during periods of prolonged metabolic stress.

Materials and Methods

Mice. A murine PACAP clone (BAC19607) was isolated from a 129 mouse genomic library (Genome Systems, St. Louis) by

Abbreviations: PACAP, pituitary adenylate cyclase-activating polypeptide; VIP, vasoactive intestinal polypeptide; ir, immunoreactivity; TH, tyrosine hydroxylase; CgA, chromogranin A; GAPDH, glyceraldehyde-3-phosphate dehydrogenase; IML, intermediolateral; VAChT, vesicular acetylcholine transporter; PNMT, phenylethanolamine *N*-methyltransferase; Q-RT-PCR, quantitative reverse transcription–PCR.

¶To whom reprint requests should be addressed. E-mail: eiden@codon.nih.gov.

The publication costs of this article were defrayed in part by page charge payment. This article must therefore be hereby marked "*advertisement*" in accordance with 18 U.S.C. §1734 solely to indicate this fact.

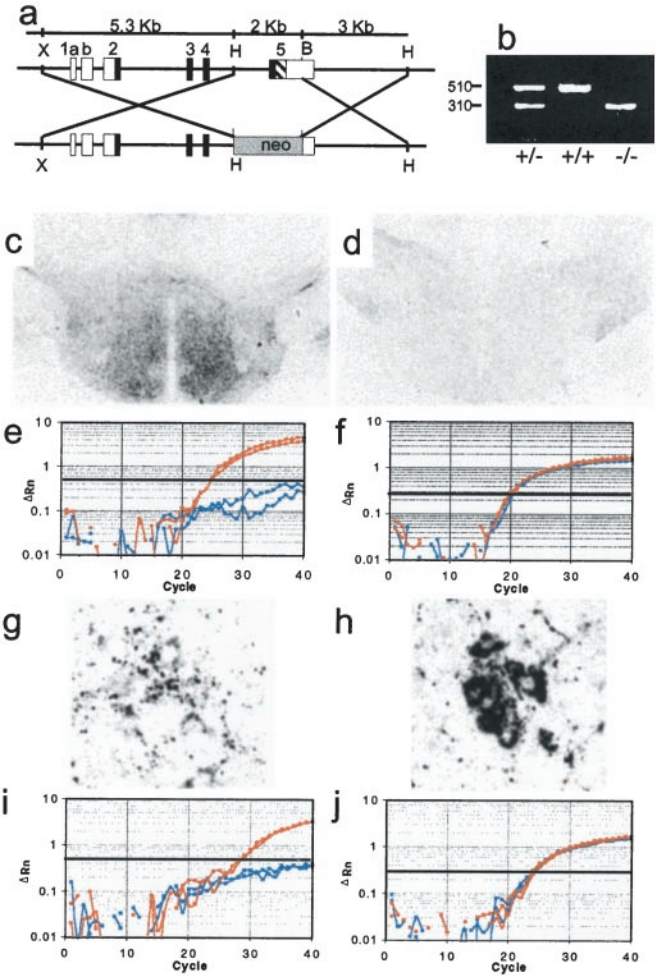

Fig. 1. Production of PACAP-deficient mice. (*a*) Design of the vector for recombination in embryonic stem cells resulting in excision of PACAP-coding sequences from the PACAP gene. Exons 1–5 are labeled; shown in black are the coding regions; the black hashed portion of exon 5 represents the PACAP ORF. *Hin*dIII (H), *Xba*I (X), and *Bam*HI (B) sites are shown. (*b*) PCR of tail DNA from wild-type, heterozygous, and homozygous F_2 mice; wild-type allele 510 bp, knock-out allele 310 bp. (*c*) PACAP-immunoreactivity (ir) staining of hypothalamus in $+/+$ F_2 mice. (*d*) PACAP-ir staining of hypothalamus in $-/-$ F_2 mice. (*e*) Q-RT-PCR of hypothalamic cDNA for PACAP from $+/+$ F_2 mice in red and $-/-$ F_2 mice in blue. (*f*) Q-RT-PCR of hypothalamic GAPDH cDNA from $+/+$ F_2 mice in red and $-/-$ F_2 mice in blue. (*g*) Weak PACAP-ir staining of preganglionic sympathetic neurons in intermediolateral column of $+/+$ mice. (*h*) VAChT-ir staining of preganglionic sympathetic neurons in adjacent section of intermediolateral column to that stained for PACAP in *g*. (*i*) Q-RT-PCR of spinal cord PACAP cDNA from $+/+$ F_2 mice in red and $-/-$ F_2 mice in blue. (*j*) Q-RT-PCR of spinal cord GAPDH cDNA from $+/+$ F_2 mice in red and $-/-$ F_2 mice in blue.

using an oligomer for the PACAP ORF within the fifth exon of the PACAP gene as a probe. A PACAP-targeting vector was constructed by first subcloning two PACAP gene *Hin*dIII fragments (a 5.3-kb fragment including exons 1–4 and a 5-kb fragment including exon 5) into a shuttle vector to generate restriction sites for insertion of a 5.0-kb *Not*I–*Xho*I fragment (including exons 1–4 of the PACAP gene) upstream of the phosphoglycerate kinase (PGK) promoter–neomycin-resistance gene and a 3.0-kb *Xba*I–*Kpn*I fragment (including exon 5 downstream of the PACAP ORF and a portion of intron 5) upstream of the PGK promoter–thymidine kinase gene, in the pPNT vector (Fig. 1). The targeting vector was linearized with *Not*I and introduced into J1 129 mouse embryonic stem cells by electroporation. Clones were selected for homologous recombination by treatment with G418 and ganciclovir. Homologous recombination was confirmed by PCR and Southern blotting. Recombination of the targeting vector with the PACAP gene locus results in the excision of the PACAP ORF from the locus (Fig. 1). Embryonic stem cells, from an embryonic stem cell clone with a recombinant PACAP allele confirmed by Southern blotting, were microinjected into C57BL/6 blastocysts to generate male chimeric offspring, which were mated with female C57BL/6 mice to generate F_1 offspring. F_1 heterozygous siblings produced $+/+$ and $-/-$ F_2 mice, group-paired for experimentation; and F_2 homozygous wild-type or null siblings were bred (F_2 $+/+$ $\times$ F_2 $+/+$ and F_2 $-/-$ $\times$ F_2 $-/-$) for generation of F_3 homozygous wild-type or null mice.

Surgical Preparation. Experimental procedures were approved by the National Institute of Mental Health Animal Care and Use Committee. Under Avertin anesthesia (tribromoethanol, 0.3 mg/g i.p.), a microrenathane catheter (MRE-025 connected to MRE-040, inner volume 15–20 μl, Braintree Scientific) was implanted into the carotid artery, sutured in place, exteriorized at the nape, and anchored by using tape. Mice recovered overnight without food. In some experiments, catheters were implanted under pentobarbitol anesthesia (50 mg/kg i.p.) and used for sampling 30 and 120 min later.

Insulin Treatment. In catheterized mice, 100 μl of blood was collected through PE20 tubing into heparinized tubes at baseline (-1 h) and at 2 and 4 h later. Heparinized saline (100 μl) was reinfused after each sample. Mice received insulin (2 units/kg) or saline (0.5 ml per mouse, i.p.) at time 0 (1 h after baseline). Plasma aliquots were stored at -80°C until assayed for catecholamines. Mice were killed by cervical dislocation, and adrenal glands were removed and stored at -80°C until analyzed. In experiments not requiring cannulation, male or female mice were fasted overnight and then treated with 1–10 units of insulin per kg or saline i.p. Whole blood (30 μl) was collected from mouse tail snips into EDTA-coated tubes at baseline and at 1, 2, and 4 h after insulin i.p. For prevention of insulin-induced mortality, PACAP (10 nmol per mouse, i.p.) was administered once, and glucose (20 μg per mouse) was administered hourly, beginning at the time of insulin injection.

Catecholamine, Glucose, Tyrosine Hydroxylase (TH), and Glucocorticoid Assays. Catecholamines were assayed by electrochemical detection after perchloric acid extraction, alumina purification, and reversed-phase liquid chromatography as described (19). Glucose was measured in 10 μl of plasma by the glucose oxidase method (Beckman glucose analyzer), or from 5 μl of whole blood by using ACCU-Check glucose test strips (Roche). Plasma glucocorticoids were measured by RIA (ICN). TH activity was measured after adrenal homogenization by using a tritiated water release method (20), with modifications (21). The TH assay was performed as described, using 10 μl of adrenal supernatant and 1.0 mM 6-methyl-5,6,7,8-tetrahydropterine (6-MPH_4) cofactor.

Quantitative PCR. For quantitative reverse transcription–PCR (Q-RT-PCR), total RNA was purified (RNAqueous kit, Ambion), DNA was removed with DNase I, and cDNA was prepared (SuperScript First Strand Synthesis, Life Technologies). Real-time quantitative PCR was performed on cDNA from 0.2 μg of total RNA (*Taq*-Man 7700 sequence detection system, Applied Biosystems) by using 90 nM primers and 150 nM probe. RNA levels were corrected for variations in amount of input mRNA with the glyceraldehyde-3-phosphate dehydrogenase (GAPDH) cDNA signal. Probes and primers used were as follows: mCgAf, GTGCGTCCTGGAAGTCATCTC; mCgAr, GGATCCTCTC-

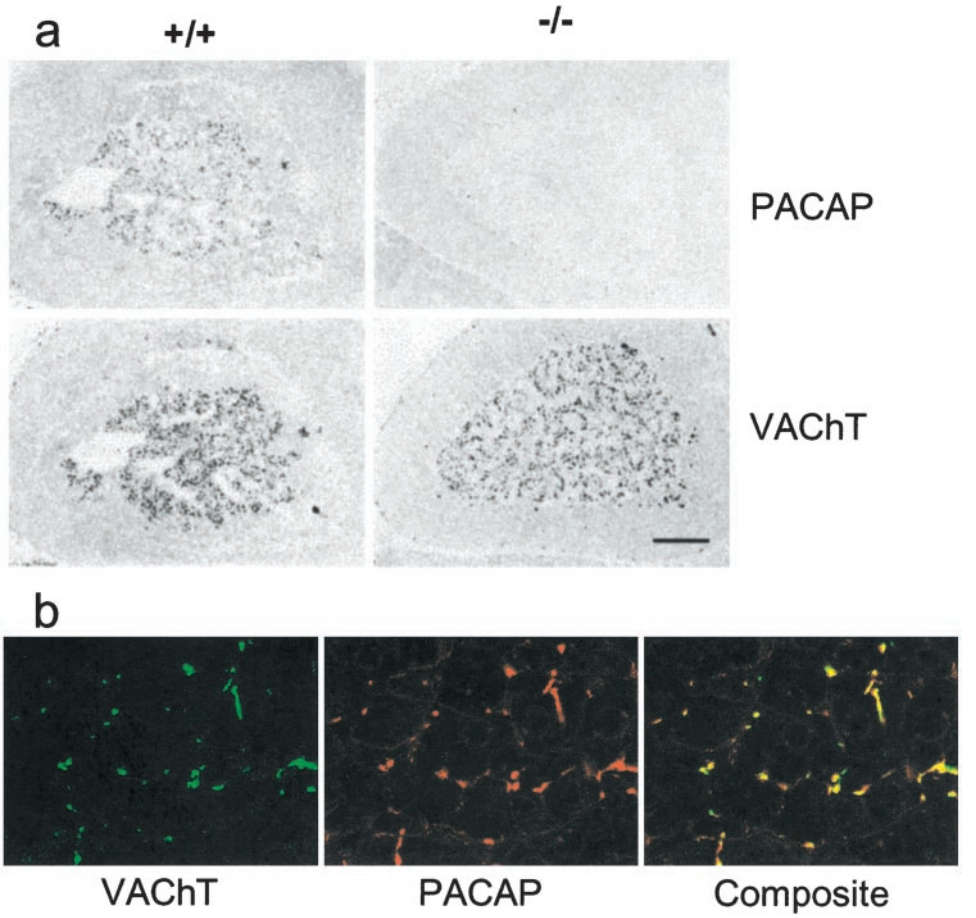

Fig. 2. Colocalization of VAChT and PACAP in adrenal medulla. (*a*) Staining for PACAP and VAChT in wild-type (+/+) and knock-out (−/−) mice. (Scale bar = 150 μm.) (*b*) Confocal microscopy for VAChT and PACAP costaining of wild-type mouse adrenal medulla. (×425.)

GTCTCCTTGGA; mCgAp, 6FAM-CAGCCCCATGCCTGTCAGCC-TAMRA; mPACAPf, CTTCACAGATAGCTACAGCCGC; mPACAPr, GGCAGCTGATCTGCTACAAGTATG; mPACAPp, 6FAM-CGCCAAGTATTTCTTGACAGCCATTTGTTTT-TAMRA; mTHf, TCCTCACCTATGCACTCACCC; mTHr, ATGTCCTGGGAGAACTGGGC; and mTHp, 6FAM-AGCCAGACTGCTGCCACGAGCTG-TAMRA, in which 6FAM represents 6-carboxyfluorescein and TAMRA represents *N,N,N′,N′*-tetramethyl-6-carboxyrhodamine. Rodent GAPDH primers and probe were from Applied Biosystems.

Immunohistochemistry. Mice were perfused under anesthesia with 10% formalin or Bouin–Hollande fixative in PBS and tissues postfixed in Bouin–Hollande. Fresh tissue was immersion fixed in Bouin–Hollande fixative (22). For single peroxidase immunostaining vesicular acetylcholine transporter (VAChT) antibody 80259, raised in rabbit against the rat/mouse sequence CEDDYNYYSRS as described (23), was used at a dilution of 1:2,000 and rabbit anti-PACAP-38 (Progen, Heidelberg) at 1:30,000. For double fluorescence fiber staining in the adrenal gland, goat anti-mammalian VAChT (VAChTcom) antibody was used with rabbit anti-PACAP-38 (24) at 1:600 and 1:2,000. For chromaffin cell staining, polyclonal sheep anti-TH (Chemicon), polyclonal rabbit anti-phenylethanolamine *N*-methyltransferase (PNMT; Eugene Tech International, Richfield Park, NJ), and polyclonal rabbit anti-chromogranin A (CgA) (anti-WE14) were used (22) at 1:400, 1:500, and 1:500, respectively. Primary antibodies were incubated overnight at 37°C. Red fluorescence was visualized with indocarbocyanine (Cy3)-conjugated anti-sheep IgG (Dianova, Hamburg, Germany), diluted 1:200 and applied for 45 min at 37°C. Green fluorescence was visualized with biotinylated secondary antibodies against rabbit IgG followed by incubation with Alexis 488-conjugated streptavidin (Mobi-Tec, Göttingen, Germany) for 2 h at 37°C. Sections were analyzed with the Olympus Fluoview confocal laser scanning microscope (Olympus, New Hyde Park, NY), and color confocal images were printed with a digital color printer (Olympus) or digitized.

Results

Generation of PACAP-Deficient Mice and PACAP Localization in the Adrenal Medulla. Generation of PACAP-deficient mice by excision of the PACAP-coding region by recombination at the PACAP gene locus (Fig. 1*a*) was confirmed by the presence of only the PACAP allele in −/− homozygous mice, the presence of only the normal allele in wild-type littermates, and the presence of both alleles in heterozygous mice, by PCR (Fig. 1*b*). PACAP-38-positive fibers were numerous in the hypothalamus of wild-type mice and absent from −/− littermates (Fig. 1 *c* and *d*). PACAP mRNA was likewise absent from hypothalamus of knock-out mice but present at relatively high levels (≈3% of the abundance of the GAPDH housekeeping gene transcript) (Fig. 1 *e* and *f*) in wild-type mouse hypothalamus. PACAP-38 immunoreactivity also was present in neurons of the intermediolateral column (IML) of the spinal cord (Fig. 1*g*) costaining with VAChT (Fig. 1*h*) but was absent from IML of knock-out mice (not shown). PACAP mRNA transcripts were detected in spinal cord of wild-type but not knock-out mice (Fig. 1 *i* and *j*).

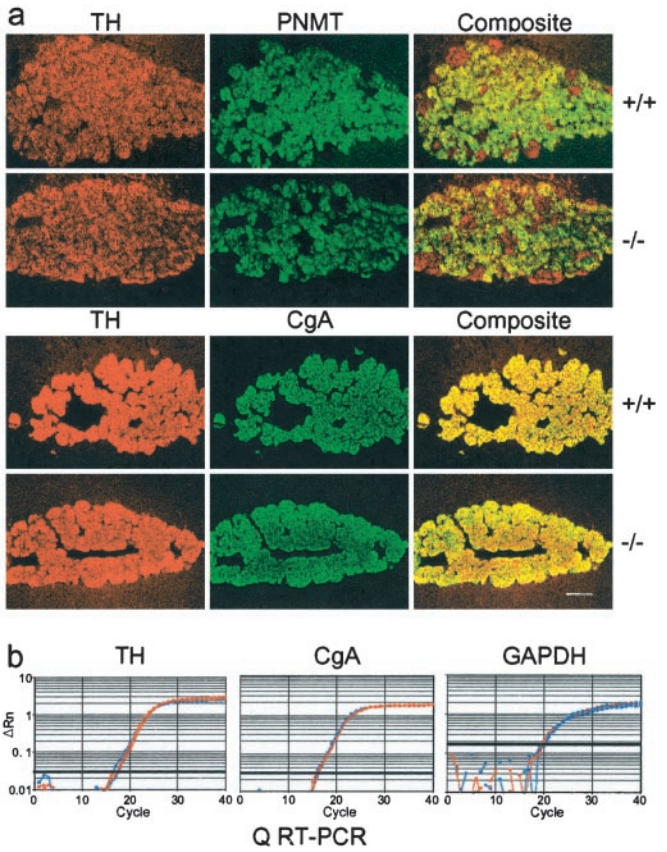

Fig. 3. Adrenal morphology. (*a*) Comparison of TH, PNMT, and CgA staining in wild-type and knock-out adrenal gland. (Scale bar = 150 μm.) (*b*) Comparison of CgA, TH, and GAPDH cDNA by Q-RT-PCR in wild-type and knock-out mouse adrenal medulla cDNA $+/+$ F_2 mice in red and $-/-$ F_2 mice in blue.

Establishing the specificity of PACAP-38 staining as wholly derived from the PACAP gene product allows the unambiguous localization of PACAP-38 to preganglionic cells of the IML, to their projections to autonomic ganglia (not shown), and to the adrenal medulla (Fig. 2*a*). PACAP-38 immunoreactivity was coextensive with that for VAChT in the adrenal medulla of the mouse, indicating that essentially all cholinergic adrenomedullary synapses are PACAPergic (Fig. 2*b*) and suggesting a general role for PACAP in sympathoadrenal function.

Sympathoadrenal Axis Morphology. The chemical neuroanatomy of the sympathoadrenal axis was compared in mice homozygous for either the wild-type or mutant PACAP allele. The expression of chromaffin cell-specific proteins including TH, PNMT, and CgA was normal in PACAP-deficient mice (Fig. 3*a*). Density and distribution of preganglionic cholinergic innervation in the adrenal medulla also were unchanged in PACAP-deficient mice (see Fig. 2*a*). The abundances of transcripts for both CgA and TH were similar in wild-type and knock-out adrenal medulla (Fig. 3*b*). Thus, a trophic role for PACAP in regulating the basal expression of proteins involved in catecholamine synthesis or packaging appears unlikely.

Response to Metabolic Stress in PACAP-Deficient Mice. Adrenomedullary response to metabolic stress was examined by treatment of mice with 1–10 units/kg insulin (i.p.), which induces hypoglycemia triggering splanchnic nerve stimulation, intense and prolonged adrenomedullary catecholamine secretion, and compensatory elevation of plasma glucose because of epinephrine-stimulated gluconeogenesis, predominantly in liver (25, 26).

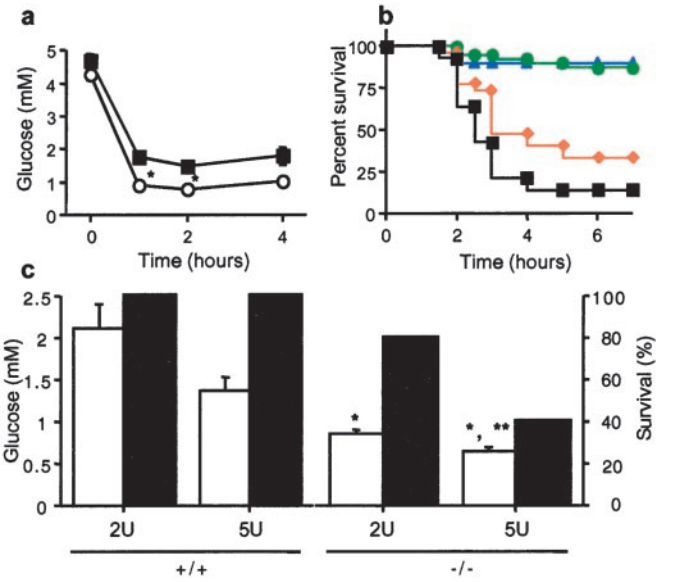

Fig. 4. Involvement of PACAP in adrenomedullary responsiveness to metabolic stress. (*a*) Insulin-induced hypoglycemia, $+/+$ (■) vs. $-/-$ (○), time course after 5 units/kg insulin. *, $P < 0.001$ relative to $+/+$ by one-way ANOVA. (*b*) Lethality dose–response curve for PACAP $-/-$ mice, 1–10 units/kg insulin, combined male and female mice: blue triangles, 1 unit; green circles, 2 units; red diamonds, 5 units; and black squares, 10 units. The $+/+$ mice are not shown; survival was 100% at all doses. (*c*) Bar graphs of plasma glucose (open bars; at 2 h, $n = 7$–9), and percentage survival (filled bars; at 4 h), $+/+$ vs. $-/-$, after administration of insulin at 2 or %5 units/kg. *, $P < 0.001$ relative to $+/+$; **, $P < 0.05$ relative to $-/-$ at 2 units of insulin, by one-way ANOVA with Scheffé's post-hoc test.

There was a more profound decrease (Fig. 4*a*) and a delayed correction in plasma glucose levels (data not shown) in response to insulin in PACAP-deficient mice, and a dose-related lethality with 1–10 units/kg insulin, correlated with hypoglycemia, that was not observed in wild-type mice (Fig. 4 *b* and *c*). Consistent with the correlation of lethality and plasma glucose after insulin in PACAP-deficient mice, 100% of $-/-$ mice coadministered glucose survived a dose of 5 units/kg insulin (data not shown). Coadministration of PACAP-38 also decreased insulin-induced lethality in PACAP-deficient mice (Fig. 5). These results support the view that the vulnerability of PACAP-deficient mice to insulin shock is a direct effect of the failure to compensate for hypoglycemia and that this deficiency is due to the immediate lack of PACAP, rather than indirect developmental or systemic effects of PACAP deficiency.

In view of the potential role of PACAP within the hypothalamo-pituitary-adrenal axis and the effects of corticosterone

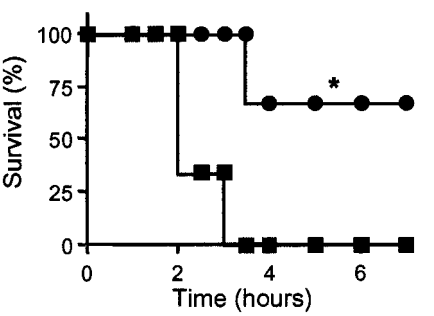

Fig. 5. PACAP-38 rescue from insulin-induced lethality in PACAP-deficient mice: ●, PACAP-38 10 nmol; ■, saline. *, $P < 0.05$ relative to saline by Kaplan–Meier rank test.

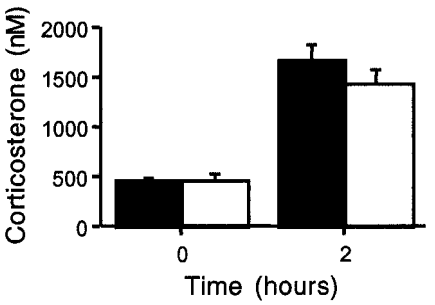

Fig. 6. Lack of change in plasma corticosterone induction after insulin (5 units/kg), +/+ (filled bars) vs. −/− (open bars).

on glucohomeostasis, plasma corticosterone levels were examined. The diurnal rhythm of plasma corticosterone at rest was equivalent in PACAP-deficient and wild-type mice (209.8 ± 50.7, 210.9 ± 79.0 nM nadir, 1,993.9 ± 284.8, 1,831.4 ± 290.6 nM peak for +/+ and −/−, respectively). Both groups showed a similar rise in plasma corticosterone after insulin administration, demonstrating that the acute responsiveness of the hypothalamo-pituitary-adrenal axis was unimpaired in PACAP-deficient mice (Fig. 6).

Plasma Epinephrine and Adrenomedullary Epinephrine and TH Responses to Insulin in PACAP-Deficient Versus Wild-Type Mice. The regulation of catecholamine synthesis and secretion *in vivo* in adult mice was investigated, using a method developed for direct collection of arterial blood from the mouse (see *Materials and Methods*). Thirty minutes after catheterization while under pentobarbital anesthesia, plasma epinephrine levels were 333 ± 54 pM for +/+ and 256 ± 38 pM for −/− mice. Two hours after catheterization, epinephrine values were 300 ± 38 and 246 ± 32 pM (+/+ and −/− mice, respectively). Epinephrine content of adrenal medulla was 17.27 ± 2.43 and 18.15 ± 0.74 nmol per gland for wild-type and PACAP knock-out mice, respectively. A role for PACAP in maintaining ambient plasma epinephrine levels and adrenomedullary content is, therefore, not supported by these data.

Plasma glucose and epinephrine were measured in fasted, conscious mice with arterial cannulae before and 1 and 3 h after insulin or saline administration (Fig. 7 *a* and *b*). Hypoglycemia was more profound in PACAP-deficient mice, and plasma epinephrine levels were lower both after fasting and after insulin compared with wild-type mice. Adrenomedullary epinephrine levels were lower after insulin only in PACAP-deficient mice (Fig. 7*c*), suggesting an impairment in compensatory catecholamine biosynthesis. Wild-type mice treated with insulin exhibit, along with increased epinephrine secretion, a prompt induction of TH, the rate-limiting enzyme in catecholamine biosynthesis. Consistent with the failure to maintain adrenomedullary epinephrine stores, TH induction was not seen after insulin in PACAP-deficient mice (Fig. 7*d*). Thus, PACAP appears to be wholly responsible for the immediate induction of TH that provides the compensatory increase in catecholamine biosynthesis required for long-term epinephrine secretion during periods of metabolic stress.

Discussion

A neuroanatomical perspective to determine the neurotransmitter function of PACAP in the mouse was developed by examining PACAP-38 immunohistochemical staining in wild-type mice and assuring its specificity by the absence of staining in their PACAP-null mutant counterparts. We used a highly specific PACAP-38 antibody along with a goat antibody against the specific cholinergic marker VAChT (24). PACAP was colocalized with VAChT in IML cell bodies in the thoracic spinal cord, and PACAP-positive fibers also showed near-complete overlap with VAChT at cholinergic synapses in the adrenal medulla of the mouse. Thus PACAP is present in the relevant anatomical configuration to be a cotransmitter along with acetylcholine in

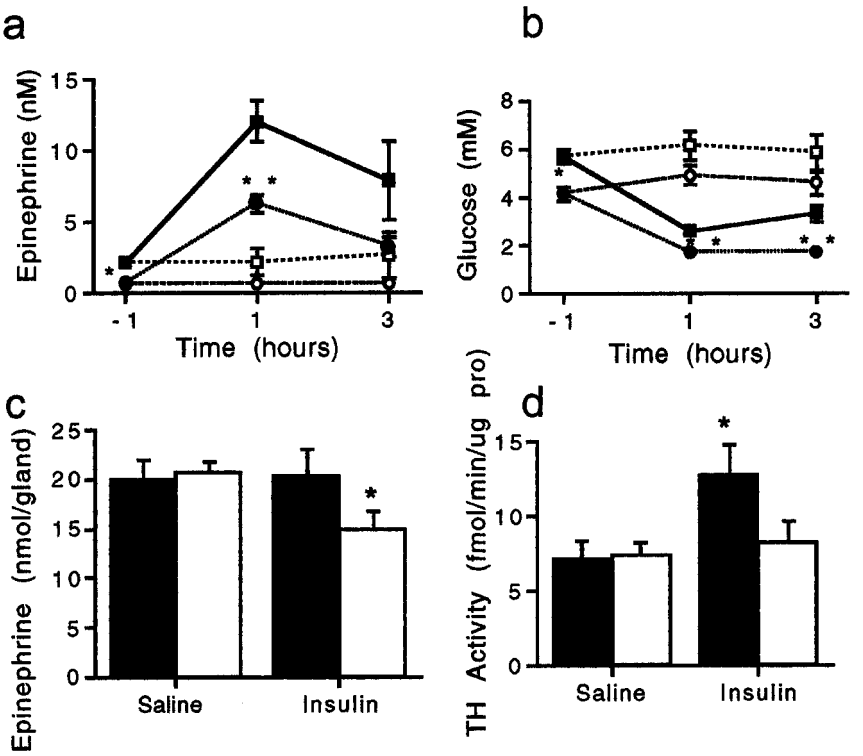

Fig. 7. Plasma epinephrine and glucose after insulin shock in PACAP-deficient vs. wild-type mice. (*a*) Plasma epinephrine levels after insulin: ■, +/+ 2 units of insulin per kg; ●, −/− 2 units of insulin per kg; □, +/+ saline; and ○, −/− saline. *, $P < 0.05$; **, $P < 0.001$ relative to +/+ by one-way ANOVA with Scheffé's post-hoc test. (*b*) Blood glucose levels after insulin: ■, +/+ 2 units of insulin per kg; ●, −/− 2 units of insulin per kg; □, +/+ saline; and ○, −/− saline. *, $P < 0.05$; **, $P < 0.001$ relative to +/+ by one-way ANOVA with Scheffé's post-hoc test. (*c*) Adrenal epinephrine levels 4 h after 2 units of insulin per kg or saline: filled bars, +/+; and open bars, −/−. *, $P < 0.05$ relative to +/+ by one-way ANOVA with Scheffé's post-hoc test. (*d*) TH is not induced in PACAP knock-out adrenal medulla 4 h after 2 units of insulin per kg: filled bars, +/+; and open bars, −/−. *, $P < 0.05$ relative to +/+ saline by one-way ANOVA with Scheffé's post-hoc test.

the splanchnic nerve innervating the adrenal gland, as suggested by previous observations in the rat (27–30).

The adrenal medulla of the PACAP-deficient mouse was normal based on several neuroanatomical markers. Immunohistochemical staining for the catecholamine-synthesizing enzymes, PNMT and TH, revealed no differences from the wild-type mouse. The intensity and distribution of cholinergic inputs visualized by staining for VAChT were similar in knock-out and wild-type mice. Staining for CgA, the major secretory protein of the adrenal medulla, was also normal in intensity and distribution. These data do not support a role for PACAP in maintaining the basic catecholaminergic and secretory phenotype of the chromaffin cell; nor did we observe developmental defects in other nervous or endocrine tissues, despite a hypothesized role for PACAP in autonomic and central nervous system development (12, 31).

Basal adrenomedullary secretory function also appeared normal in PACAP-deficient mice with plasma levels of epinephrine equivalent to wild type in anesthetized mice. However, in response to a metabolic stress, the mice lacking the PACAP gene were unable to survive. PACAP knock-out mice had a more profound hypoglycemia than wild-type mice both in response to an overnight fast and after an i.p. bolus injection of insulin. The initial epinephrine secretory response after insulin was preserved, but the total secretory response was significantly diminished, demonstrating a critical role for PACAP in the maintenance of adrenomedullary epinephrine secretion in the face of prolonged metabolic stress. Our *in vivo* data are wholly consistent with the ability of PACAP, but not acetylcholine, to maintain continuous catecholamine secretion from the perfused rat adrenal gland at levels achievable by splanchnic nerve stimulation (7, 17).

We therefore tested the hypothesis that the failure in glucose regulation after insulin in PACAP-deficient mice was secondary to impaired catecholamine synthesis leading to exhaustion of releasable catecholamine stores. Adrenomedullary epinephrine content examined 4 h after insulin revealed diminished stores in the null mutant mice. To rule out the contributions of other glucoregulatory hormones, corticosterone was measured after the insulin treatment. Both wild-type and PACAP knock-out mice exhibited a robust response in plasma corticosterone to the insulin challenge, suggesting that the inability to counterregulate insulin-induced hypoglycemia in the PACAP-deficient mice is primarily because of a defect in catecholamine synthesis.

Induction of TH activity is a hallmark of stress responses mediated through splanchnico-adrenomedullary synapse activation (32, 33). PACAP, in addition to stimulating catecholamine secretion, potently activates TH in chromaffin cell cultures (34–35). Consistent with these *in vitro* studies, PACAP-deficient mice failed to respond to insulin with an induction of TH enzymatic activity.

The present findings provide a physiological context for previous observations that PACAP and related peptides mimic, in perfused adrenal gland or adrenomedullary cells in culture, the sustained catecholamine secretion, and compensatory stimulation of catecholamine biosynthesis, that follows sustained splanchnic nerve firing during long-term metabolic stress (7, 34, 36) PACAP, in keeping with a general role for neuropeptides in stress and disease (37), thus performs an emergency response function in the paraphysiological regulation of the sympathoadrenal axis during metabolic stress.

We thank Dennis Murphy for consultation on experimental design, Graeme Eisenhofer, Derek LeRoith, and Juan Saavedra for critically reviewing this report, David Huddleston and Emily Shepard for excellent technical assistance, William Gwin for PCR measurements, and Ed Ginns for consultation and assistance in generating PACAP-deficient mice. This work was supported in part by the Volkswagen Foundation and Deutsche Forschungsgemeinschaft Grant SFB297.

1. Guidotti, A., Mao, C. C. & Costa E. (1973) in *Frontiers in Catecholamine Research,* eds. Usdin, E. & Snyder, S. (Pergamon, Oxford), pp. 231–236.
2. Wakade, A. R. (1998) *Adv. Pharmacol.* **42,** 595–598.
3. Douglas, W. W. & Rubin, R. P. (1961) *J. Physiol. (London)* **159,** 40–57.
4. Mueller, R. A., Thoenen, H. & Axelrod, J. (1970) *Eur. J. Pharmacol*. **10,** 51–56.
5. Malhotra, R. K. & Wakade, A. R. (1987) *J. Physiol. (London)* **383,** 639–652.
6. Malhotra, R. K., Wakade, T. D. & Wakade, A. R. (1988) *Neuroscience* **26,** 313–320.
7. Wakade, A. R. (1988) *J. Neurochem.* **50,** 1302–1308.
8. Watanabe, T., Masuo, Y., Matsumoto, H., Suzuki, N., Ohtaki, T., Masuda, Y., Kitada, C., Tsuda, M. & Fujino, M. (1992) *Biochem. Biophys. Res. Commun.* **182,** 403–411.
9. Wakade, T. D., Blank, M. A., Malhotra, R. K., Pourcho, R. & Wakade, A. R. (1991) *J. Physiol. (London)* **444,** 349–362.
10. Inoue, M., Fujishiro, N., Ogawa, K., Muroi, M., Sakamoto, Y., Imanaga, I. & Shioda, S. (2000) *J. Physiol. (London)* **528,** 473–487.
11. Holgert, H., Holmberg, K., Hannibal, J., Fahrenkrug, J., Brimijoin, S., Hartman, B. K. & Hökfelt, T. (1996) *NeuroReport* **8,** 297–301.
12. Arimura, A. (1998) *Jpn. J. Physiol.* **48,** 301–331.
13. Malhotra, R. K., Wakade, T. D. & Wakade, A. R. (1989) *J. Neurosci.* **9,** 4150–4157.
14. Fukushima, Y., Hikichi, H., Mizukami, K., Nagayama, T., Yoshida, M., Suzuki-Kusaba, M., Hilsa, H., Kimura, T. & Saton, S. (2001) *Am. J. Physiol*. **281,** R1562–R1567.
15. Chowdhury, P. S., Guo, X., Wakade, T. D., Prywara, D. A. & Wakade, A. R. (1994) *Neuroscience* **59,** 1–5.
16. Isobe, K., Nakai, T. & Takuwa, Y. (1993) *Endocrinology* **132,** 1757–1765.
17. Guo, X. & Wakade, A. R. (1994) *J. Physiol. (London)* **475,** 539–545.
18. Jamen, F., Persson, K., Bertrand, G., Rodriguez-Henche, N., Puech, R., Bockaert, J., Ahren, B. & Brabet, P. (2000) *J. Clin. Invest.* **105,** 1307–1315.
19. Holmes, C., Eisenhofer, G. & Goldstein, K. S. (1994) *J. Chromatogr. B Biomed. Sci. Appl.* **653,** 131–138.
20. Reinhard, J. F., Smith, G. K. & Nichol, C. A. (1986) *Life Sci.* **39,** 2185–2189.
21. Hooper, D., Kawamura, M., Hoffman, B., Kopin, I. J., Hunyady, B., Mezey, E. & Eisenhofer, G. (1997) *J. Chromatogr. B Biomed. Sci. Appl.* **694,** 317–324.
22. Schäfer, M. K.-H., Nohr, D., Romeo, H., Eiden, L. E. & Weihe, E. (1994) *Peptides* **15,** 263–279.
23. Weihe, E., Tao-Cheng, J. H., Schäfer, M. K. H., Erickson, J. D. & Eiden, L. E. (1996) *Proc. Natl. Acad. Sci. USA* **93,** 3547–3552.
24. Weihe, E. & Eiden, L. E. (2000) *FASEB J.* **14,** 2435–2449.
25. Connolly, C. C., Ivy, R. E., Adkins-Marshall, B. A., Dobbins, R. L., Neal, D. W., Williams, P. E. & Cherrington, A. D. (1996) *Diabetes Res. Clin. Pract.* **31,** 45–56.
26. Cantu, R. C., Correll, J. W. & Manger, W. M. (1968) *Proc. Soc. Exp. Biol. Med.* **129,** 155–161.
27. Beaudet, M. M., Braas, K. M. & May, V. (1998) *J. Neurobiol.* **36,** 325–336.
28. Chiba, T., Tanaka, K., Tatsuoka, H., Dun, S. L. & Dun, N. J. (1996) *Neurosci. Lett.* **214,** 65–68.
29. Frödin, M., Hannibal, J., Wulff, B. S., Gammeltoft, S. & Fahrenkrug, J. (1995) *Neuroscience* **65,** 599–608.
30. Sundler, F., Ekblad, E., Hannibal, J., Moller, K., Zhang, Y. Z., Mulder, H., Elsas, T., Grunditz, T., Danielsen, N., Fahrenkrug, J., *et al.* (1996) *Ann. N.Y. Acad. Sci.* **805,** 410–428.
31. Waschek, J. A., Cassillas, R. A., Nguyen, T. B., DiCicco-Bloom, E. M., Carpenter, E. M. & Rodriguez, W. I. (1998) *Proc. Natl. Acad. Sci. USA* **95,** 9602–9607.
32. Thoenen, H., Mueller, R. A. & Axelrod, J. (1969) *Nature (London)* **221,** 1264.
33. Sterling, C. R. & Tank, A. W. (2001) *J. Pharmacol. Exp. Ther.* **296,** 15–21.
34. Ruis, A. R., Guidotti, A. & Costa, E. (1994) *Life Sci.* **54,** 1735–1743.
35. Marley, P. D., Cheung, C. Y., Thomson, K. A. & Murphy, R. (1996) *J. Auton. Nerv. Syst.* **60,** 141–146.
36. Wakade, A. R., Wakade, T. D. & Malhotra, R. K. (1988) *J. Neurochem.* **51,** 820–829.
37. Hökfelt, T., Broberger, C., Xu, Z. D., Sergeyev, V., Ubink, R. & Diez, M. (2000) *Neuropharmacology* **39,** 1337–1356.